Insect Biochemistry and Molecular Biology 173 (2024) 104165

Contents lists available at ScienceDirect

Insect Biochemistry and Molecular Biology

journal homepage: www.elsevier.com/locate/ibmb

# Physiological and transcriptional changes associated with obligate aestivation in the cabbage stem flea beetle (*Psylliodes chrysocephala*)

Gözde Güney [a,*], Doga Cedden [b], Johannes Körnig [c,d], Bernd Ulber [a], Franziska Beran [c,d], Stefan Scholten [e], Michael Rostás [a,**]

[a] Agricultural Entomology, Department of Crop Sciences, University of Göttingen, D-37077, Göttingen, Germany
[b] Department of Evolutionary Developmental Genetics, Johann-Friedrich-Blumenbach Institute, GZMB, University of Göttingen, D-37077, Göttingen, Germany
[c] Department of Insect Symbiosis, Max Planck Institute for Chemical Ecology, D-07745, Jena, Germany
[d] Population Ecology Group, Friedrich Schiller University, D-07743, Jena, Germany
[e] Division of Crop Plant Genetics, Department of Crop Sciences, University of Göttingen, D-37075, Göttingen, Germany

ARTICLE INFO

*Keywords:*
Flea beetle
Summer diapause
Transcriptomics
Life cycle
Insect physiology
RNA-Seq

ABSTRACT

Aestivation is a form of seasonal dormancy observed in various insect species, usually coinciding with the summer season. The cabbage stem flea beetle, *Psylliodes chrysocephala* (Coleoptera: Chrysomelidae), is a key pest of oilseed rape that obligatorily aestivates as adult in late summer. Since the physiological and transcriptional processes linked to aestivation in *P. chrysocephala* are still little understood, we analyzed relevant physiological parameters and performed RNA-seq analyses on laboratory-reared beetles in their pre-aestivation, aestivation, and post-aestivation stages. We found that the beetles reached aestivation at 15 days post-eclosion, showing strongly reduced metabolic activity, with less than 50% $CO_2$ production, compared to pre-aestivating individuals. Under constant laboratory conditions, the beetles aestivated for about 25 days. Female beetles reached reproductive maturity at a median of 52 days post-eclosion. Furthermore, aestivating beetles had significantly reduced carbohydrate reserves and increased lipid reserves compared with pre-aestivating beetles, indicating that aestivation is associated with drastic changes in energy metabolism. Aestivating beetles contained 30% less water and their survival rates under high-temperature conditions (30 °C) were 40% higher compared to pre-aestivating beetles. RNA-seq studies showed that, in particular, gene ontology terms related to carbohydrate and lipid metabolism, digestion, and mitochondrial activity were enriched, with clear differences in transcript abundance between beetles in aestivation compared to pre- or post-aestivation. Specifically, mitochondrial transcripts, such as *respiratory chain I subunits*, and digestion-related transcripts, such as *trypsin*, were less abundant during aestivation, which supports the idea that aestivation is associated with decreased metabolic activity. This study represents the first exploration of the transcriptomic and physiological processes linked to aestivation in *P. chrysocephala*.

## 1. Introduction

Diapause in insects is characterized by a predetermined cessation of development during immature stages or the absence of reproductive activity in adults. It is also characterized by a reduction in metabolic rate and behavioral activity (Denlinger, 2002; Schiesari and O'Connor, 2013). Aestivation is a type of diapause that typically occurs during the summer season as opposed to the winter hibernation observed in many temperate insect species (Saulich and Musolin, 2018; Storey and Storey, 2012). Both winter diapause and aestivation are dormant states in anticipation of unfavorable conditions rather than a direct response to unfavorable conditions, which is a feature of quiescence (Gill et al., 2017). Diapause is either induced by environmental conditions (facultative diapause) or is genetically determined (obligate diapause). Facultative diapause is prevalent among insects and is primarily triggered by token stimuli such as a decrease in photoperiod or temperature. In contrast, the less common obligatory diapause occurs at a genetically predetermined stage in the species' life cycle, regardless of prevailing

* Corresponding author.
** Corresponding author.
*E-mail addresses:* ggueney@uni-goettingen.de (G. Güney), michael.rostas@uni-goettingen.de (M. Rostás).

https://doi.org/10.1016/j.ibmb.2024.104165
Received 15 April 2024; Received in revised form 25 July 2024; Accepted 25 July 2024
Available online 30 July 2024

environmental conditions (Denlinger, 2022). However, the survival success of this inactive phase relies on its synchronization with unfavorable seasonal conditions (Gill et al., 2017). Hence, obligate diapause is predominantly observed in univoltine species, where the life cycle of each generation is synchronized with unfavorable seasonal conditions. In contrast, multivoltine species generally exhibit facultative diapause as only some generations need to undergo diapause (Numata and Shintani, 2023).

Both obligate and facultative diapause are usually preceded by a diapause preparation phase in which the insect exhibits various adaptive behaviors to enhance the likelihood of survival during the subsequent dormant phase, such as migrating to protective areas and increasing feeding (Denlinger, 2002; Koštál, 2006). The feeding period allows the accumulation of energy reserves such as triglycerides and glycogen (Cedden et al., 2024c; Hahn and Denlinger, 2011; King et al., 2020), which can be catabolized to maintain energy homeostasis during diapause. For instance, *Colaphellus bowringi* adults reared under long-day conditions accumulate lipids to fuel their aestivation (Tan et al., 2017; Zhu et al., 2019). Similarly, *Leptinotarsa decemlineata* adults exposed to short-day conditions accumulate large amounts of lipids to be catabolized during winter diapause (Güney et al., 2021). Additionally, insects entering diapause may upregulate the production of protective agents to cope with harsh environmental conditions. For instance, heat shock proteins can protect the cell against the accumulation of misfolded proteins under stress conditions such as high temperatures encountered during diapause (Rinehart et al., 2007; Sømme, 1964). Additionally, enhanced production of glycerol can increase an insect's resistance to freezing in low temperatures (Hayward et al., 2005; Kojić et al., 2018). Furthermore, previously accumulated energy reserves can support post-diapause development, migration, or reproduction (Sinclair, 2015; Sinclair and Marshall, 2018).

A large number of RNA-seq studies have compared diapausing and non-diapausing stages of insects (Hao et al., 2019; Kang et al., 2016; Kankare et al., 2016; Lebenzon et al., 2021; Ren et al., 2018). However, studies on obligatory aestivation are scarce due to the facultative and winter-occurring nature of the majority of the diapause responses in insects. A rare example of an insect that obligatorily enters diapause during summer is *Galeruca daurica* (Coleoptera: Chrysomelidae) (Zhou et al., 2019). A transcriptomics study on *G. daurica* found evidence for the regulation of various metabolic pathways, including fatty acid biosynthesis during the transition into and out of the aestivation (Yan et al., 2021). These results suggest that the physiological changes associated with diapause are regulated at the transcriptional level, albeit studies directly linking them are scarce.

The cabbage stem flea beetle, *Psylliodes chrysocephala* (Coleoptera: Chrysomelidae) is a major pest of winter oilseed rape (*Brassica napus* subsp. *napus*) in northern Europe. The management of this pest became challenging due to emergence of insecticide resistance populations and the ban on neonicotinoids, which prompted the investigation of alternative management strategies, including RNA interference (Cedden et al., 2024a). Adults of *P. chrysocephala* inflict damage on oilseed rape plants by feeding on leaves, while larvae mine in stems and petioles (Ortega-Ramos et al., 2022; Williams, 2010). After emerging in early summer, adult *P. chrysocephala* engages in a brief period of intensive feeding before entering aestivation until August/September, usually seeking out sheltered areas like woodlands and hedgerows (Ankersmit, 1964). Aestivating beetles neither feed nor reach reproductive maturity until aestivation is completed in 1–2 months. Subsequently, beetles invade newly sown oilseed rape fields to feed on cotyledons or young leaves and oviposit in soil cracks located near the host plant (Bonnemaison and Jourdheuil, 1954; Ortega-Ramos et al., 2022). Given the obligate nature of aestivation in *P. chrysocephala* (Säringer, 1984), the adult stage can be categorized into three phases, namely pre-aestivation (newly emerged adults), aestivation, and post-aestivation.

To enhance our understanding of the mechanisms underlying aestivation in this economically important flea beetle species, we examined the physiological and transcriptional dynamics involved in this process. We hypothesized that aestivation is linked to various physiological and transcriptional changes that modulate cellular metabolism, alter body composition, and enhance stress tolerance under summer conditions in diapausing *P. chrysocephala*. Hence, we monitored carbon dioxide emission, energy reserves, and reproductive maturity across pre-aestivation, aestivation, and post-aestivation stages. We also identified differentially abundant transcripts in females between these stages and conducted enrichment analyses using a functionally annotated *de novo* transcriptome assembly. Lastly, we analyzed transcript abundance patterns to further elucidate the findings from the enrichment analyses.

## 2. Materials and methods

### 2.1. Insect culture

*Psylliodes chrysocephala* was reared on potted oilseed rape plants (*Brassica napus* 'Marathon') in BugDorm-2120 rearing tents (60 x 60 × 60 cm; BugDorm, Megaview Science Co., Ltd., Taichung, Taiwan) as described in Cedden et al. (2024b). The laboratory culture of *P. chrysocephala* was first established by Franziska Beran in 2012 using adults collected in Laasdorf, Thuringia, Germany, and field-collected adults or larvae were introduced almost every year to maintain genetic diversity. The tents were kept under controlled conditions at 20 ± 2 °C and 65.5 ± 10% relative humidity with a 16:8 h light-dark cycle. The light was provided by daylight spectrum LED lamps (Bioledex GoLeaf E2, DEL-KO). To obtain insects at different ages, newly emerged adult beetles were kept in groups of 15–20 individuals in ventilated PET boxes (11 x 6 × 15 cm) with detached oilseed rape leaves under the conditions described above. The females were distinguished from males based on tarsal morphology (Kaufmann, 1941).

### 2.2. Carbon dioxide emission

Carbon dioxide emission rates ($VCO_2$) of female and male beetles (n = 16 per sex) were recorded using an LI-820 $VCO_2$ Gas Analyzer (LI-COR Environmental GmbH, Bad Homburg, Germany) at 5-day intervals for 60 days following adult emergence. A single beetle was placed into a 35 mL glass vial with a controlled air supply from a mini air pump (Luftpumpe LP27-06, 6V, ≥1.5 L/min, ≤430 mA; DAYPOWER, Germany). Prior to each assessment, the air was purified of excess $CO_2$ using a soda lime filter ($Ca(OH)_2$) (Dräger, Lübeck, Germany) to establish a stable baseline. Upon stabilization, the system's valves were sealed and $CO_2$ levels were monitored over a 15-min interval. $CO_2$ detection and data conversion were conducted using a LI-820 $CO_2$ Gas Analyzer connected to a Multifunction I/O Device (USB-6008; National Instruments, Germany), with digital conversion of the $CO_2$ data facilitated through LabVIEW software (v14.0.1; National Instruments). The difference in $CO_2$ concentration ($[\Delta CO_2]$) was calculated by subtracting the 5-min $CO_2$ levels from those at 15 min. This value was then normalized against the observation time and the mass of the beetle, which was measured using a Sartorius MC5 micro-balance (Sartorius AG, Göttingen, Germany) immediately before starting the $CO_2$ tests (adapted from Cedden et al., 2024b). The weight corrected $\Delta CO_2$ ppm values were analyzed using two-way ANOVA followed by Bonferroni's multiple comparison test (GraphPad Prism v10.0).

### 2.3. Reproductive maturation

Ovaries were dissected from 5, 25, and 45-day-old females (n = 8) in phosphate-buffered saline (7.4 pH) to assess morphological changes. The selected time points were based on preliminary observations of ovaries at 5-day intervals for a period of 60 days post-emergence (n = 4). The ovaries were found undeveloped until 40 days post-emergence, while maturation was observed only in 45-day-old females. The dissected ovaries were examined under a Leica TL3000 Ergo stereo

microscope (Microsystems, Switzerland) and photographed using a Leica DMC5400 camera. The area of each ovariole per female was measured using ImageJ (v1.53t, https://imagej.nih.gov/ij/index.html). The average ovariole areas per female were statistically analyzed using one-way ANOVA followed by Tukey's test (GraphPad Prism v10.0).

Oviposition activity was investigated by placing newly emerged individual female and male beetles (n = 14 pairs) into plastic boxes containing fresh oilseed rape leaf discs that were replenished every two days. The adult pairs were monitored daily for the presence of eggs to reveal the beginning of the oviposition period. Data analysis involved

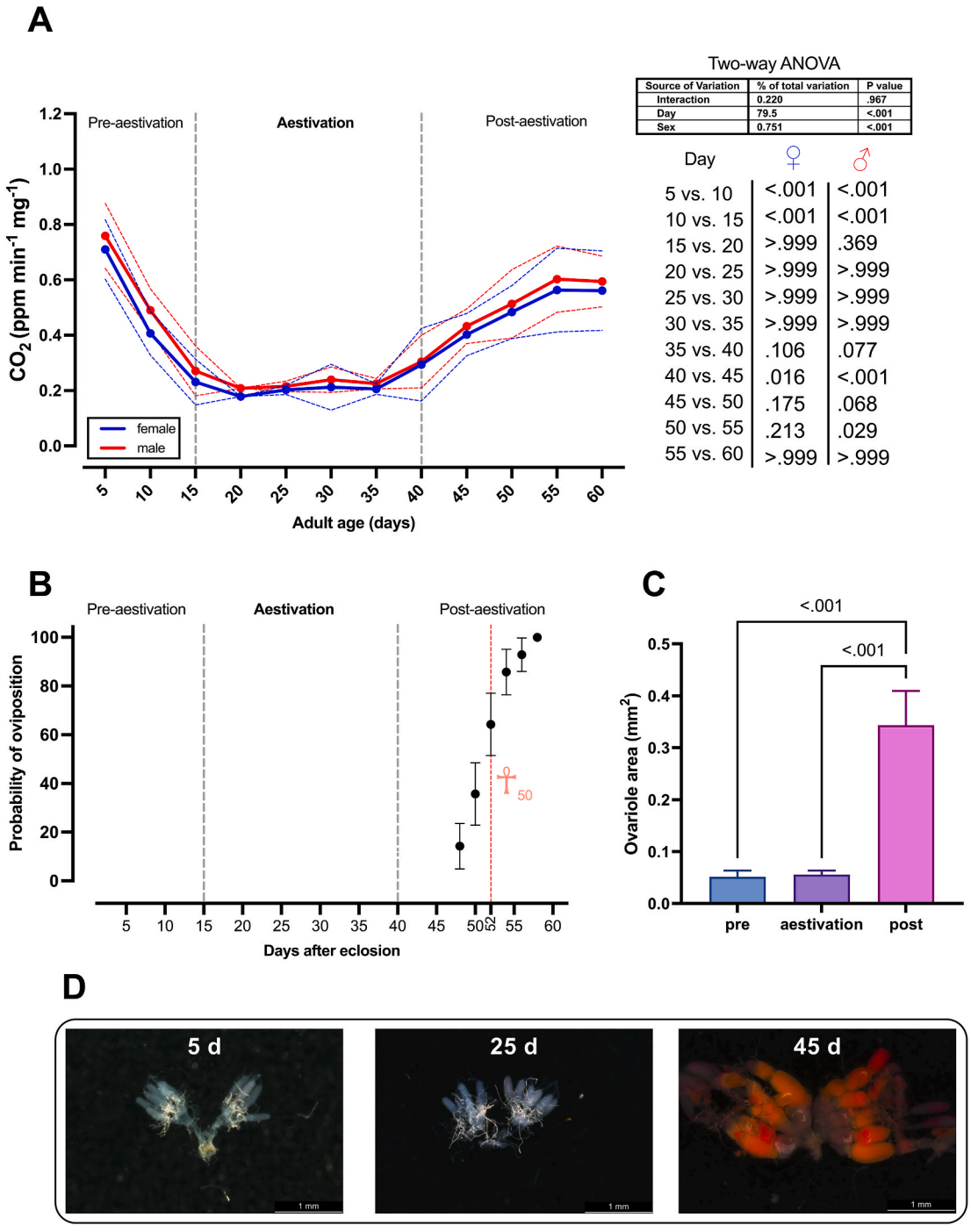


**Fig. 1.** Characterizing the aestivation period in *P. chrysocephala*. (A) $VCO_2$ production (ppm min$^{-1}$ mg$^{-1}$) of *P. chrysocephala* females (blue) and males (red) over 60 days at 5-day intervals following adult emergence. The line graph depicts the mean $VCO_2$ production for each sex, with dotted lines indicating the standard deviation (n = 16 per sex). A two-way ANOVA with the factors of day and sex was performed. The table presents the percentage of explained variation and *P* values for day, sex, and their interaction. Bonferroni's multiple comparison tests were employed to compare $VCO_2$ production at each time point with the subsequent time point. Adjusted *P* values are given for females and males separately. (B) Cumulative probability of oviposition in female beetles, when paired with male beetle's post-adult emergence (n = 14, one pair per Petri dish). Kaplan-Meier analysis determined the day at which half the population is expected to have started oviposition ($\text{♀}_{50}$). The error bars indicate the standard error of the probability (C) Mean ± SD ovariole areas (mm$^2$) in pre-aestivating (pre; 5 days old), aestivating (25 days old), and post-aestivating (post; 45 days old) females (n = 8). Tukey's test compared ovariole areas, with significant differences ($P \leq 0.05$) indicated above bars. (D) Representative images of ovaries examined at different time points following adult emergence (n = 8).

plotting a Kaplan-Meier curve, with the laying of the first eggs serving as the endpoint. The median female age at first oviposition was calculated using GraphPad Prism v10.0.

### 2.4. Survival under heat stress

Pre-aestivating adults (initially 5 days old) and aestivating adults (initially 30 days old) were kept at 30 °C and 60% relative humidity, maintaining the regular 16:8 h light-dark cycle. Survival was monitored daily for 6 days (n = 30). Fresh leaf discs (approx. 130 $mm^2$) punctured from the first true leaves of randomly selected oilseed rape plants (growth stage BBCH 30–35) were provided to both groups every two days. Survival curves were plotted using the Kaplan–Meier method. The *P* value and hazard ratio (hazard in pre-aestivation vs. hazard in aestivation) were calculated by the log-rank test using GraphPad Prism v10.0.

### 2.5. Composition of energy reserves and water content

Body composition analyses were performed to determine the contents of energy reserves in 5, 30, and 55 days old female and male beetles (n = 6–10 per sex). The 5-day-old female represented the active and newly emerged state. The 30-day-old female represented the middle of aestivation, while the 55-day-old female represented post-aestivation with 15 days of active time following aestivation termination, according to the $VCO_2$ pattern (Fig. 1A). At the designated time points, the beetles were frozen with liquid nitrogen and kept at −80 °C following fresh weight measurements. Total protein, total lipid, glycogen, and soluble carbohydrate contents were measured using a previously established method by Foray et al. (2012) with minor modifications described in Sporer et al. (2021). This method enables the quantification of major energy reserves in individual beetles. In addition, water contents were assessed using another batch of female and male beetles (n = 10 per sex) by first measuring individual fresh weights before freezing them with liquid nitrogen and letting the samples dry at 60 °C for 72 h to measure the dry weights, which were subtracted from the initial fresh weights. Measurement results for each content were analyzed using two-way ANOVA, with one of the factors being sex and the other being the adult stage (Table S1). Tukey's test was conducted to investigate the differences between the three stages.

### 2.6. cDNA library

Total RNA from pre-aestivating (5 days old), aestivating (30 days old), and post-aestivating (55 days old) female beetles were extracted using the Quick-RNA Tissue/Insect Kit (Zymo Research, Freiburg, Germany). Subsequently, the RNA samples were purified using the TURBO DNA-free™ kit (Thermo Fisher Scientific, Waltham, MA, USA). To eliminate sex-related variability, only female beetles were sampled. RNA integrity was verified using an Agilent 2100 Bioanalyzer and an RNA 6000 Nano Kit (Agilent Technologies, Santa Clara, CA, USA). RIN values ≥ 7.0 were considered appropriate for mRNA library preparation. In total, 10 libraries (4, 3, and 3 libraries respectively per pre-aestivation, aestivation, and post-aestivation stages) were prepared using NEBNext® Poly(A) mRNA Magnetic Isolation Module followed by NEBNext kit (E7490, NEB, Ipswich, MA, USA). The quality and quantity of the libraries were checked on an Agilent 2100 Bioanalyzer using the Agilent DNF-935 Reagent Kit (Agilent Technologies, Santa Clara, CA, USA). Libraries were pooled to equimolar amounts, and a total concentration of 3.4 ng/μL was obtained. Sequencing was performed by BGI Genomics Tech Solutions Co. Ltd (Hong Kong) on a DNBSEQ-T7 platform. The total reads in all libraries were 374 million, ranging from 13 million to 66 million (see Table S2 for details). Raw read files were deposited in the Sequence Read Archive (SRA) database of NCBI under the accession numbers: SAMN33022552 - SAMN33022561.

### 2.7. De novo assembly and functional annotation

Erroneous k-mers from paired-end reads were removed using Rcorrector (v1.0.5) with default options (Song and Florea, 2015), and unfixable reads were discarded using the "FilterUncorrectabledPEfastq.py" function in Transcriptome Assembly Tools (Song and Florea, 2015). Adaptor sequences were removed, and reads with a quality score greater than 30 were retained using TrimGalore! (v0.6.7). The cleaned reads (n = 3 per three adult phases) were assembled *de novo* using Trinity with default options. In total, 224 million bases were assembled covering 341,670 transcripts, including putative isoforms (https://doi.org/10.6084/m9.figshare.21922938). The d*e novo* assembly had an N50 value of 1532 and a BUSCO (v5.4.2) completeness score of 96.7% when compared against the Endopterygota lineage (BUSCO.v4 datasets). Putative isoforms were combined to obtain a supertranscriptome containing 189,229 transcripts in total. The supertranscriptome was deposited at GenBank as a Transcriptome Shotgun Assembly (TSA) under the accession number GKIH01000001:GKIH01098921 (NCBI BioProject: PRJNA930726).

The transcriptome (including isoforms) was annotated using Trinotate (v3.2.2). This tool combines the outputs of various packages, such as NCBI BLAST+ (v2.13.0; nucleotide and predicted protein BLAST), TransDecoder (v5.5.0; coding region prediction), SignalP (v4.0; signal peptide prediction) (Petersen et al., 2011), TmHMM (v2.0; transmembrane domain prediction) (Krogh et al., 2001), and HMMER (v3.3.2; homology search) into an SQLite annotation database. The uniprot_sprot (04/2022) and pfam-A (11/2015) databases were downloaded using Trinotate and the default E-value thresholds were used during the searches with BLAST+ and HMMER. The obtained annotation database was used to extract gene ontology (GO) terms associated with individual transcripts using the "extract_GO_assignments_from_Trinotate_xls.pl" whereas the signals and TmHMM outputs were manually extracted using Excel spreadsheets. The longest protein-coding regions in the supertranscriptome data predicted by TransDecoder were subjected to Kyoto Encyclopedia of Genes and Genomes (KEGG) pathway annotation via GhostKoala v2.2 (https://www.kegg.jp/ghostkoala/).

### 2.8. Differential transcript abundance

Read counts per transcript were calculated using Salmon (v1.9) by mapping the cleaned reads onto our *de novo* transcriptome. Transcripts with less than 15 total read counts across all 10 libraries were discarded from further analysis. The R package "DeSeq2 "(v4.2) was used to identify the differentially abundant transcripts in the aestivation vs. pre-aestivation and aestivation vs. post-aestivation comparisons. Transcripts with *P* values below 0.05 and $Log_2$ Fold change (LFC) values below −1.0 or above 1.0 were accepted as significantly increased or decreased in abundance, respectively.

### 2.9. Enrichment analyses

The "enricher" function in the R package" ProfileClusterer" was used to analyze the enrichment status of GO terms and KEGG pathways associated with the differentially abundant transcripts in the two pairwise comparisons. All the transcripts with at least one GO annotation served as the background (12,410 transcripts). We did not distinguish between increase and decrease in transcript abundance during the enrichment analyses due to the ambiguous nature of the GO term annotations. We plotted the top 35 most significantly enriched GO terms (differentially abundant transcripts and full enrichment results are available at https://doi.org/10.6084/m9.figshare.24085815).

The dataset was also investigated for the number of transcripts predicted with signal peptides, transmembrane domains, both, or neither. The number of transcripts belonging to each category was determined by manually investigating the SQLite annotation database, and Chi-

squared tests were performed to compare the proportion of each category among differentially abundant transcripts with that among the background transcripts. Here, the transcripts that increased or decreased in abundance were separately analyzed, and Bonferroni correction was applied ($P < 0.05/18 = 0.002$).

Transcript hits from significantly enriched GO terms coinciding with our physiological measurements were selected for the visualization of their abundance pattern across the three adult stages. R v4.3 was used to Z-normalize the transcript abundance and GraphPad Prism v10.0 was used to construct the heat maps. The names of the transcripts were extracted from the annotation database and the names were curated where necessary.

## 3. Results

### 3.1. Physiological characterization of aestivation

#### 3.1.1. Metabolic rates

To estimate the timing of aestivation in our laboratory *P. chrysocephala* population, we measured the metabolic rate (ppm $mg^{-1}$ $min^{-1}$) of female and male adults every 5 days from day 5 to day 60 post-emergence. The metabolic rate changed significantly over time, with the day factor alone explaining 79.5% of the variation (Fig. 1A). In addition, the metabolic rate of males was significantly higher than that of females ($P < 0.001$), but there was no significant interaction between the sex and day factors ($P = 0.967$). Metabolic rate decreased between days 5 and 15, remained stable until day 40, and increased thereafter. These results confirm that *P. chrysocephala* adults undergo an obligatory aestivation phase that lasts for about 25 days.

#### 3.1.2. Reproductive maturation

Subsequently, we investigated the reproductive maturity of females by analyzing the onset of oviposition under our laboratory conditions and by comparing the morphology of the reproductive system of females in the pre-aestivation, aestivation, and post-aestivation phases. The onset of oviposition ranged from day 48 to day 60 after emergence in the post-aestivation phase. The median onset of oviposition, i.e. the time when half of the female population had started oviposition, was estimated to be day 52 (Fig. 1B). In agreement with this observation, we found that the ovariole area was significantly larger in post-aestivating females compared to pre-aestivating and aestivating females ($P < 0.001$), while no clear morphological differences were found between pre-aestivating and aestivating females (Fig. 1C and D). In contrast to females, no clear morphological changes were observed in the reproductive system of males between the pre-aestivation, aestivation, and post-aestivation phases. (Fig. S1).

#### 3.1.3. Survival under heat stress

To test whether pre-aestivating and aestivating adults are differentially affected by high temperature, we exposed pre-aestivating and aestivating adults to 30 °C and 60% relative humidity. As expected, aestivating adults survived significantly better than pre-aestivating adults ($P = 0.009$; Fig. 2). The hazard ratio between pre-aestivating and aestivating was 2.7, indicating that pre-aestivating adults are more strongly affected by high temperature than aestivating adults.

#### 3.1.4. Composition of energy reserves and water content

To further characterize the physiological changes associated with aestivation in *P. chrysocephala*, we compared the allocation of energy reserves and water content of pre-aestivating, aestivating, and post-aestivating males and females (Fig. 3A). Protein concentration did not differ between the three stages in females but was significantly lower in post-aestivating males than in pre-aestivating males ($P < 0.04$).

In contrast to protein levels, lipids, glycogen, and water-soluble carbohydrate (WSC) concentrations differed significantly between aestivating and non-aestivating phases in both sexes. While lipid concentrations were significantly higher during aestivation compared to the pre-aestivation phase ($P < 0.05$), glycogen and WSC concentrations were significantly lower. In the post-aestivation phase, the lipid concentrations were significantly lower, whereas the glycogen and WSC concentrations remained at a similar level as in the pre-aestivation phase (Fig. 3B, C, 3D). In addition, we observed a significantly lower WSC concentration in males compared to females, whereas protein, lipid, and glycogen concentrations did not differ between both sexes.

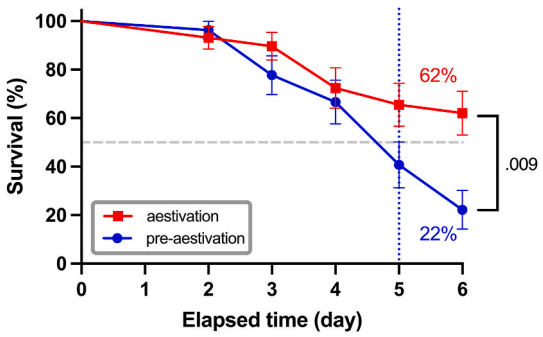


**Fig. 2.** Survival of pre-aestivating and aestivating *P. chrysocephala*. Pre-aestivating and aestivating adults were reared at 30 °C and 60% relative humidity to simulate heat stress. Survival was monitored daily. The survival curves show the mean percentage of surviving adults ± standard error (n = 30) calculated by the Kaplan–Meier estimator. The *P* value was calculated by log-rank test. The blue vertical line indicates the median lethal time of the pre-aestivating adults.

Water content was significantly lower in aestivating beetles compared to pre- and post-aestivating beetles. In addition, post-aestivating females had a significantly lower water content than pre-aestivating females (Fig. 3E). Taken together, our results show that aestivation is associated with drastic changes in the composition of energy reserves and water content in *P. chrysocephala*.

### 3.2. Transcriptional characterization of aestivation

#### 3.2.1. Differentially abundant transcripts

Using our RNA-seq reads and *de novo* transcriptome assembly, we performed two pairwise comparisons; aestivation vs. pre-aestivation and aestivation vs. post-aestivation. (Fig. S2). The latter stage (the stage after "vs.") was taken as the reference for each comparison. The aestivation vs. pre-aestivation comparison revealed that 3013 and 3223 transcripts were increased and decreased in abundance, respectively, among the 34,368 transcripts that passed the pre-filtering. Similarly, 2762 and 3876 transcripts were increased and decreased in abundance, respectively, in the aestivation vs. post-aestivation comparison. Hence, about 5% of transcripts were differentially abundant depending on the adult stage. To determine the transcripts that were specifically increased and decreased in abundance during aestivation, we checked the overlap between the two comparisons. The overlap analysis resulted in 246 and 657 transcripts that were significantly increased and decreased in abundance in aestivation compared to pre- and post-aestivation stages, respectively, indicating a bias toward decrease in abundance (2.7-fold compared to increase in abundance) in this filtered dataset.

#### 3.2.2. Enrichment analyses

The top enriched GO terms in the aestivation vs. pre-aestivation comparison (emphasizing the initiation of aestivation) were mainly related to cellular metabolism (Fig. 4A). The analysis showed alterations in carbohydrate metabolism and mobilization. Additionally, we observed alterations in mitochondrial activity, e.g., mitochondrial electron transport (GO:0006120), tricarboxylic acid cycle (GO:0006099), and mitochondrial respiratory chain complex I and IV terms (GO:0005747 and GO:0005751). The most significantly enriched

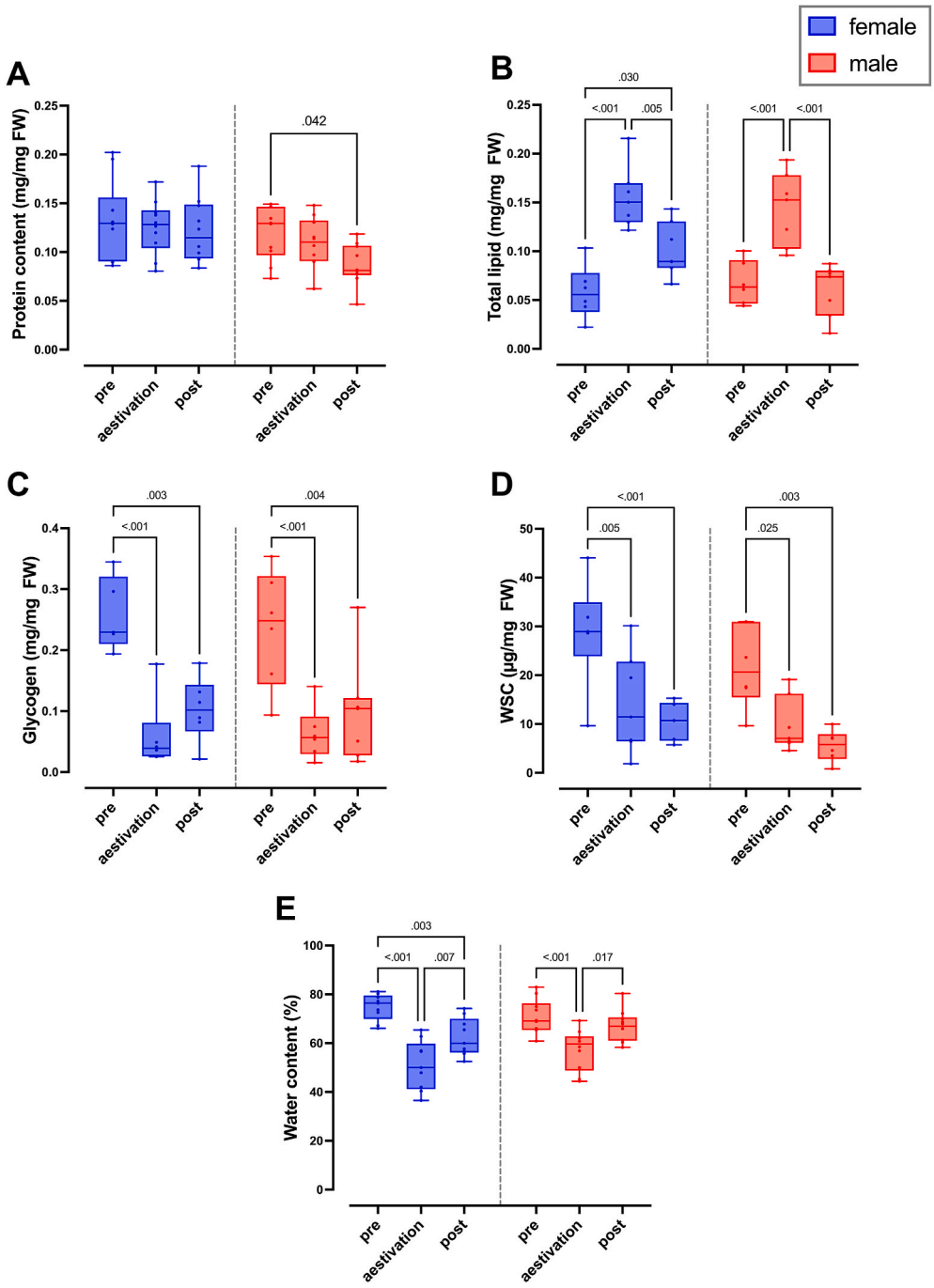


**Fig. 3.** Body composition analysis. Total protein (A), total lipid (B), glycogen (C), and water-soluble carbohydrate WSC (D), and water content (E) contents of pre-aestivating (pre; 5 days old), aestivating (30 days old), and post-aestivating (post; 55 days old) *P. chrysocephala* females (blue) and males (red). Each content was divided by the fresh weight (FW) of the associated beetle and plotted as a box plot which shows the median (middle line), upper and lower quartiles (the box), and the minimum and maximum (whiskers) of the consumption values (n = 6–10 per sex). Two-way ANOVA was conducted to test whether the factors stage (pre, aestivation, and post) and sex significantly affected each measured parameter (see Table S1). The effect of the factor stage within sex was further investigated by Tukey's test ($P \leq 0.05$).

GO term was digestion (GO:0007586), and various other terms and pathways related to this process, such as cellulose catabolic process (GO:0030,245) and polygalacturonase (GO:0004650), were also enriched. Another significantly enriched term related to metabolism was the fatty acid biosynthetic process (GO:0006633). As expected, juvenile hormone (JH) esterase (GO:0004453) activity was also significantly enriched. Terms related to chitin binding (GO:0008061) and structural constituents of cuticle (GO:0042,302) were also among the top enriched GO terms. In addition, changes in molecular functions involving iron atoms were also supported by two enriched terms (GO:0005506 and GO:0051,539).

The comparison between aestivation vs. post-aestivation revealed that regulation of digestive processes, cellular metabolism, JH esterase, and iron binding activity are associated with the termination of aestivation as well (Fig. 4B). Nonetheless, distinct terms were also enriched in this comparison. Embryonic placenta development (GO:0001892) and post-embryonic development (GO:0009791) terms are likely to be related to the reproductively mature state of post-aestivating females.

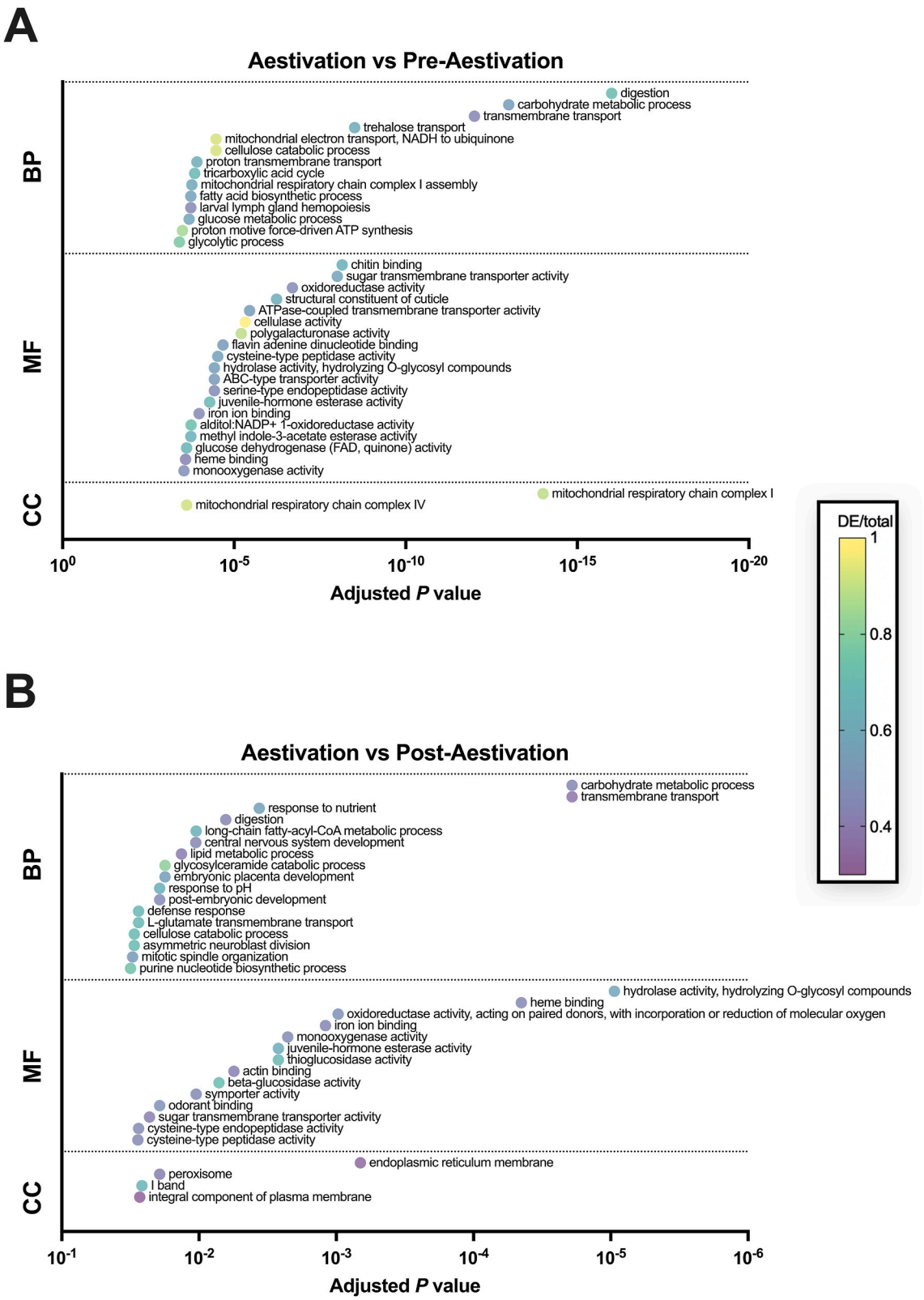


**Fig. 4.** GO term enrichment results. The bubble plots of the enrichment analysis of transcripts identified as significantly increased or decreased in abundance in the aestivation vs. pre-aestivation (A) and aestivation vs. post-aestivation (B) comparisons. The top 35 significantly enriched GO terms were shown and the terms were grouped into biological process (BP), molecular function (MF), and cellular component (CC). The X-axis indicates the adjusted *P* values of the enriched terms while the color of the bubble indicates the ratio between the differentially abundant transcripts and the total transcripts associated with each GO term.

Interestingly, response to pH (GO:0009268) and defense response (GO:0006952) were among the top enriched biological processes. The cellular components among the top enriched terms included endoplasmic reticulum membrane (GO:0005789) and peroxisome (GO:0005777), implicating their involvement in lipid metabolism and stress response. Additionally, the enrichment of the term I band (GO:0031,674), which is a muscle-related structure, hints at structural changes in muscle tissue during aestivation termination.

Using the data from pair-wise transcriptome comparisons, we investigated whether there is any bias towards transcripts with predicted signal peptides and/or transmembrane helices among differentially abundant transcripts compared to the background. The analysis revealed a significant enrichment of transcripts containing signal peptides, transmembrane helices, or both among transcripts that were decreased in abundance in both the aestivation vs. pre-aestivation and aestivation vs. post-aestivation comparisons (Fig. S3). All three categories were also significantly enriched among the transcripts that increased in abundance in the aestivation vs. post-aestivation comparison.

### 3.2.3. *Investigations at the transcript level*

To enhance clarity in interpreting enrichment analysis outcomes, such as discerning whether biological processes are activated or deactivated, we employed heat maps. The heat maps show the transcript abundance patterns of the top 20 differentially abundant transcripts that were associated with the enriched GO terms of interest (i.e., significantly enriched and related to the physiological measurements). We also included transcripts specifically regulated during aestivation to gain further insights (Fig. 5). The top terms were associated with carbohydrate and lipid metabolic processes (GO:0005975 and GO:0006629), mitochondrial respiratory chain, reproduction (embryonic development and female reproductive system terms), heme binding (GO:0020,037)

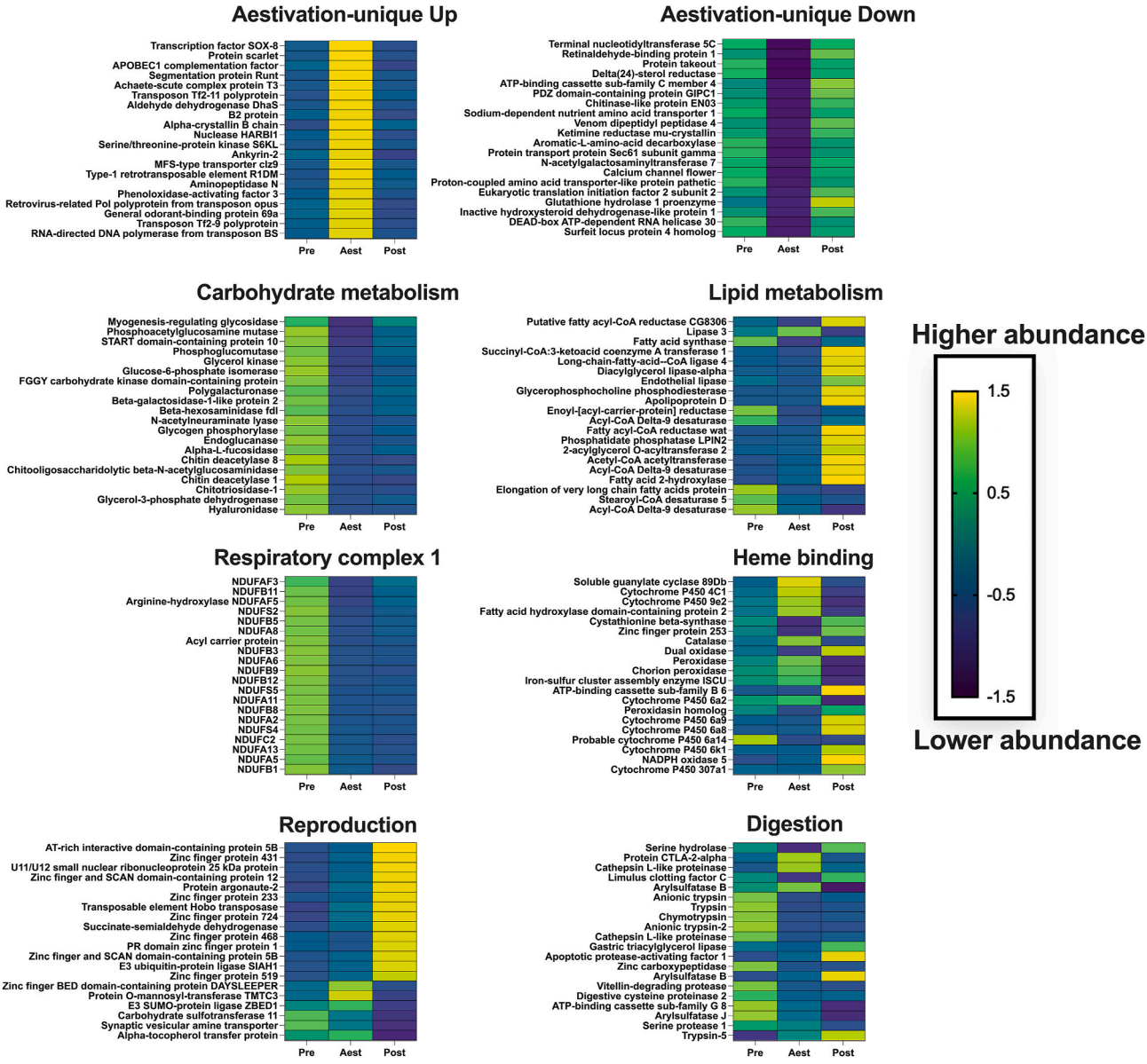


**Fig. 5.** Investigation at transcript level. Heat maps illustrating the abundance of top differentially abundant transcripts during pre-aestivation (Pre), aestivation (Aest), or post-aestivation (Post) stages of female *P. chrysocephala*. Each heatmap shows the top 20 differentially abundant transcripts from sets uniquely increased or decreased in abundance during aestivation or the GO terms of interest from Fig. 4. Each row represents a transcript with its annotation taken from our annotation database and curated where necessary (see https://doi.org/10.6084/m9.figshare.21922938 for the original automated annotations). The color of the cells represents the z-score normalized read count values averaged per stage; dark blue indicates decrease in abundance and yellow cells indicate increase in abundance.

and feeding activity (digestion and response to nutrients (GO:0007584) terms), as determined by our annotation database.

Prominent among the transcripts uniquely increased in abundance during aestivation was a transcription factor identified as *Sox-8* (DN3796_c1_g2) (Fig. 5). Additionally, a *putative pigmentation protein* (*protein scarlet*, DN17760_c0_g1) and an mRNA editing transcript (*APOBEC1 complementation factor*, DN21869_c0_g1) were among the top transcripts specifically regulated during aestivation. We also noticed multiple transposon-related transcripts to be specifically increased in abundance during aestivation. The top transcripts distinctly decreased in abundance during aestivation were associated with a range of putative functions, including protein transport and translation initiation.

The top transcripts associated with carbohydrates were especially increased in abundance during pre-aestivation and then decreased in abundance during both aestivation and post-aestivation (Fig. 5). For instance, a *glucose-6-phosphate* (DN3300_c0_g1) transcript was had the lowest abundance in aestivation. This finding is consistent with our body composition measurements. Both glycogen and WSC contents were abundant only during the pre-aestivation stage and largely absent during the following two stages.

On the other hand, important transcripts related to lipid metabolism showed a completely different pattern compared to those linked with carbohydrate metabolism (Fig. 5). Many of these transcripts, such as *apolipoprotein* (DN1435_c0_g1, lipid carriers in hemolymph) and *diacylglycerol lipase* (DN9768_c0_g1) were specifically increased in abundance during the post-aestivation stage. In contrast, the transcript related to lipogenesis, *fatty acid synthase* (DN4305_c0_g1), was increased in abundance only during pre-aestivation, presumably to accumulate the lipid reserves that peaked during aestivation according to our total lipid measurements. Also, an aestivation-specific *lipase* (DN2340_c0_g2) was identified, possibly responsible for energy and metabolic water production during aestivation through the catabolism of lipids.

As expected from the $CO_2$ measurements, transcripts associated with respiratory chain complex I were increased in abundance during pre-aestivation and dramatically decreased in abundance during aestivation, indicating metabolic suppression in the latter (Fig. 5). These transcripts included *NADH dehydrogenase [ubiquinone] 1 alpha subcomplex assembly factor 3* (DN19356_c0_g1). Interestingly, abundance levels did not return to pre-aestivation levels during post-aestivation.

Among the top differentially abundant transcripts with heme binding annotation, many *cytochrome P450s* were identified, including *4C1* (DN20570_c0_g1). Additionally, the abundance of two *peroxidases* (DN17009_c0_g1 and DN17645_c0_g1) peaked during aestivation, indicating the activation of the antioxidant defense system to support the maintenance of aestivation.

As expected, differentially abundant transcripts related to reproduction were increased in abundance in post-aestivation (Fig. 5), which is the reproductively active adult stage (Fig. 1). These transcripts mainly included the zinc finger domain containing transcripts that are likely acting as transcription regulators. Interestingly, a *putative argonaute 2* (DN6854_c0_g1) transcript, which is responsible for the defense against viruses and transposons through the RNAi pathway (Zhou and Rana, 2013), was increased in abundance only in post-aestivation.

Most of the top differentially abundant transcripts related to feeding activity, such as *trypsin* (DN105_c0_g2) and other proteinases transcripts, were increased in abundance during pre-aestivation and decreased in abundance during aestivation (Fig. 5). The increased abundance of transcripts associated with digestive activity differed between pre-aestivation and post-aestivation. Intriguingly, some of these transcripts reached their abundance peaks during aestivation, including the *cathepsin L-like proteinase* (DN4833_c0_g2).

## 4. Discussion

Aestivation represents an obligatory stage in the life cycle of *P. chrysocephala*, a key pest of winter oilseed rape in Europe (Tixeront et al., 2024; Willis et al., 2020). Despite its importance, the phenomenon of aestivation remains poorly understood, not only in *P. chrysocephala* but also in other insect pests, particularly at the molecular level. This study marks the first comprehensive characterization of aestivation in *P. chrysocephala,* examining both physiological and transcriptional aspects. We identified notable changes in cellular metabolism, mitochondrial activity, reproductive maturity, and body composition in relation to the initiation, maintenance, and termination of aestivation.

The onset of diapause is generally associated with a substantial and sustained decrease in metabolic rate (Lehmann et al., 2020; Melicher et al., 2024; Sgolastra et al., 2010). The fact that aestivation coincides with high temperatures implies that the environmental conditions do not aid the suppression of metabolism and thus might involve mechanisms that have not been described in winter-diapausing insects (Denlinger, 2022; Hahn and Denlinger, 2011). Therefore, prior to conducting the other experiments, we periodically measured the $VCO_2$ emission of *P. chrysocephala* adults to rationally select the sampling time points. We observed a significant suppression of $VCO_2$ levels beginning in 15-day--old adults, which persisted for 25 days (Fig. 1A). This 25-day period was identified as the aestivation period in our *P. chrysocephala* laboratory population. Notably, this duration was shorter than that reported in a previous study, which documented an aestivation period ranging from $48 \pm 17$ to $62 \pm 14$ days (Sáringer, 1984). We attribute this variability in reported aestivation periods to genetic and methodological differences. Sáringer (1984) used a Hungarian field-collected population of *P. chrysocephala* while we used a lab population established from a German population and the determination of the aestivation period was based on observational evidence rather than on measuring the beetle's metabolic rate, as was done in this study. Interestingly, we found that the smaller *P. chrysocephala* males had consistently higher $VCO_2$ levels than the larger females. This is in line with the metabolic scaling hypothesis, which proposes that smaller organisms have higher metabolic rates than larger ones, due to a decreasing surface-to-volume ratio (Glazier, 2015).

The results from the GO term enrichment analysis align well with the observed metabolic suppression during aestivation, as numerous mitochondria-related terms were enriched in the pre-aestivation vs. aestivation comparison (Fig. 4A). Although $VCO_2$ serves as an indirect indicator, primarily reflecting Krebs cycle activity rather than direct measurements of electron transport chain and ATP production, its suppression suggests metabolic alterations. Further investigations showed decreased in abundance of core components of the Krebs cycle, such as *NADH dehydrogenase subunits*, during aestivation (Fig. 5). Hence, considering both the $VCO_2$ and RNA-seq results, we postulate a decrease in the mitochondrial membrane potential and ATP-ADP ratio in *P. chrysocephala* aestivation. These alterations likely facilitate successful aestivation by reducing the demand on internal energy reserves, similar to the diapause in *L. decemlineata*, where mitophagy supports metabolic suppression (Lebenzon et al., 2022). According to the hygric hypothesis, suppression of metabolism indicates reduced respiration rates, which, in other species, has enabled a reduction in water loss rates (Gibbs et al., 2003; Matthews and White, 2012). The enhanced survival under summer conditions might partly be due to the reduction in desiccation risk conferred by the lower respiration rates as well as the increased in abundance of *cytochrome P450s*, such as *4C1* (Shen et al., 2021), in *P. chrysocephala*.

During aestivation, *P. chrysocephala* beetles do not feed. However, they resume feeding after aestivation, albeit at a reduced rate compared to their pre-aestivation levels (Ankersmit, 1964; Sivčev et al., 2016). Consistent with these observations, our enrichment analyses indicate decreased digestion during aestivation (Fig. 4A and B). The decrease in the abundance of transcripts associated with digestion likely represents one strategy to reduce energy expenditure on temporally unnecessary processes, a phenomenon observed, for example, in *Culex pipiens* (Robich and Denlinger, 2005), *G. daurica* (Ma et al., 2019) and *L. decemlineata* (Yocum et al., 2009). Interestingly, most of the

digestion-related and carbohydrate metabolism-related transcripts that decreased in abundance during aestivation did not return to their pre-aestivation levels upon emergence from aestivation. Additionally, some transcripts were uniquely increased in abundance in post-aestivation (Fig. 5), which might be an adaptation to the change of diet from old to young oilseed rapes (Ankersmit, 1964). The changes in the abundance of digestion-related transcripts may reflect both qualitative (different ages of oilseed rape) and quantitative (greater feeding in the pre-aestivation than post-aestivation stages) differences in the feeding patterns of the two stages.

The absence of feeding and the corresponding decreased abundance of digestion transcripts in aestivating beetles prompts the question: how do these beetles secure the requisite energy for sustaining their basal metabolism during this period? Consistent with the notion that diapausing insects draw upon their internal energy reserves (Denlinger, 2022; Hahn and Denlinger, 2007), we found evidence for metabolic alterations or the mobilization of lipids and carbohydrates during the transition into and out of aestivation at the transcriptional level (Fig. 5B). Moreover, the measured changes in lipid, glycogen, and water-soluble carbohydrate (WSC) levels also indicate that the energy reserves of the adult beetles depend on their diapause stage (Fig. 3B–D). While glycogen and WSC levels were almost completely depleted during early-mid aestivation, lipid levels were highest during aestivation and were depleted by post-aestivation. The alterations in carbohydrate metabolism and mobilization at the transcriptional level might be responsible for the depletion of glycogen and WSC levels in early to mid-aestivation. The peak in lipid levels during aestivation suggests that lipid stores continued to accumulate 5 days post-emergence (sampling time point). The overall pattern of energy store levels suggests that glycogen and WSC are primarily catabolized during early aestivation, while lipids serve as the primary metabolic fuel during mid to late aestivation. Similar dynamic changes in diapause metabolic fuel were observed in *Culex pipiens*, where the consumption of glucose and glycogen stores precedes the consumption of lipid stores (King et al., 2020; Zhou and Miesfeld, 2009). Also, aestivating *Eurygaster maura* males increased the transcript abundance of a lipolytic gene, *lipid storage droplet 1*, presumably to fuel the aestivation (Toprak et al., 2014). Additionally, one of the *cathepsin L-like proteinases* emerged as top transcripts increasing in abundance during aestivation (Fig. 5). This *proteinase* might play a role in inducing matrix *metalloproteinases*, leading to the degradation of extracellular matrix proteins. This process could potentially trigger fat body cell dissociation and activate lipid metabolism during aestivation. This *cathepsin L-like proteinase* function was observed, for example, in the pupae of the non-diapausing moth *Helicoverpa armigera* (Jia and Li, 2023). Post-aestivating adults, especially females, may heavily rely on these lipid reserves for oviposition and migration behavior (Sinclair, 2015; Sinclair and Marshall, 2018; Wolda and Denlinger, 1984). This hypothesis is supported by the observation that many lipid metabolism-related transcripts were uniquely increased in post-aestivating individuals (Fig. 5).

Previous studies have indicated that adult *P. chrysocephala* reproduces after completing aestivation (Alford, 1979; Vig, 2003). However, a comprehensive investigation is still lacking. In this study, we observed that females slowly emerged from aestivation after 35 days, as their $VCO_2$ levels increased. Yet, females did not have mature ovaries and did not oviposit until they were 45 days old (Fig. 1B and D). Likewise, most of the transcripts related to reproduction, such as reproduction-related *zinc finger-containing transcription factors*, had increased transcript abundance, specifically during the post-aestivation phase (Fig. 5).

Numerous transcriptional alterations linked to aestivation cannot be fully explored here due to space limitations. Noteworthy changes include the increase of several transcripts encoding transcription repressors (e.g., *zinc finger proteins*) and positive transcriptional regulator transcripts during aestivation compared to the pre-aestivation state. These changes likely contribute to the establishment of the aestivation phenotype through the transcriptional regulation of other relevant genes, a phenomenon observed in other diapausing insects (Bao and Xu, 2011; Guo et al., 2018; Torson et al., 2023; Zhang et al., 2020). Importantly, one specific transcription factor, annotated as *SOX-8*, showed a unique and substantial increase in abundance solely during aestivation. Insect genomes contain eight to nine *SOX-8* genes and canonically regulate developmental processes such as segmentation and neurogenesis through DNA binding activity. This particular *SOX-8* gene may have specialized to serve as a regulator of the genes that facilitate the aestivation phenotype. Future studies should prioritize its characterization to elucidate its role in mediating aestivation-related gene regulation.

The potential functions of aestivation may include synchronization with the life cycle of host plants, avoidance of predators or parasitoids, and resistance to abiotic factors associated with summer, such as high temperature and low humidity (Masaki, 1980; Saulich and Musolin, 2018). *P. chrysocephala* adults are small in size (3–4 mm) (Edde, 2022) and consequently have large surface-area-to-volume ratios, suggesting an increased risk of desiccation during the summer season (Kühsel et al., 2017). Our current study provides evidence supporting the idea that a critical function of aestivation is the mitigation of increased desiccation risk. First, the survival rate in the aestivating *P. chrysocephala* adults was higher than that of pre-aestivating adults. A similar increase in survival under high temperatures was also observed in the diapausing pupa of *Helicoverpa assulta* compared to non-diapausing stages (Liu et al., 2016). Moreover, the observed changes in the transcription of *trehalose transporter* transcripts during aestivation (Fig. 4A) may be necessary for maintaining an optimal intracellular concentration of trehalose. Some studies suggest that trehalose may act as a chemical chaperone against various stress conditions, including extreme temperatures and desiccation (Crowe, 2007; Tapia and Koshland, 2014). In addition, it serves as a significant source of energy for sustaining basal metabolism, which produces metabolic water (Kikawada et al., 2007; Zhou et al., 2022). Interestingly, the water content during aestivation was lower compared to pre- and post-aestivation stages. This was unexpected as aestivating beetles might benefit from high water content due to risk of desiccation. A possible explanation might be that accumulation of lipids causes a lower percentage of water content (Benoit and Denlinger, 2007; Tan et al., 2017), which might be compensated by the gradual metabolic water production through the oxidation of lipid stores (Arrese and Soulages, 2010). Also, lack of feeding activity might be contributing to the reduced water content in aestivation (Benoit, 2010).

Several transposon-related transcripts were specifically increased in abundance during aestivation (Fig. 5). Although similar observations have been made in various diapausing insects, such as *L. decemlineata* (Lebenzon et al., 2021), *C. pipiens* (Robich et al., 2007), and *Drosophila montana* (Kankare et al., 2016) the functional roles of these transposon-related transcripts increasing in abundance during aestivation remain to be elucidated. Indeed, there is an intriguing possibility that transposable elements are involved in the regulation of diapause/aestivation by influencing epigenetic regulatory mechanisms.

## 5. Conclusion

This study marks the first investigation into the obligatory aestivation in *Psylliodes chrysocephala* at the mRNA level, complemented by physiological data. The results suggest that newly emerged *P. chrysocephala* adults prepare for aestivation by accumulating energy reserves such as sugars and lipids and subsequently reducing their metabolic rate through reducing mitochondrial activity and decreasing transcript abundance of metabolic enzymes. This adaptation allows the insect to compensate for the lack of feeding during aestivation. To sustain their basal metabolism, beetles heavily rely on their sugar reserves such as WSC and glycogen, during the early phase of aestivation and then β-oxidize previously accumulated lipid reserves. The termination of aestivation is associated with changes in lipid metabolism and probably

*zinc finger containing transcription factors*, enabling the insect to reach reproductive maturity. Notably, our findings have identified several testable hypotheses concerning the key genes and processes underlying the transitioning into and out of aestivation in *P. chrysocephala.* Such insights hold promise for the enhancement of RNAi-based management strategies targeting this pest.

## CRediT authorship contribution statement

**Gözde Güney:** Writing – original draft, Visualization, Validation, Methodology, Investigation, Formal analysis, Data curation, Conceptualization. **Doga Cedden:** Writing – review & editing, Visualization, Software, Methodology, Formal analysis, Data curation. **Johannes Körnig:** Methodology. **Bernd Ulber:** Writing – review & editing, Supervision. **Franziska Beran:** Writing – review & editing, Supervision, Resources, Conceptualization. **Stefan Scholten:** Writing – review & editing, Supervision, Resources, Conceptualization. **Michael Rostás:** Writing – review & editing, Supervision, Resources, Conceptualization.

## Declaration of competing interest

The authors have no relevant financial or non-financial interests to disclose.

## Data availability

Data is available on Figshare and NCBI

## Acknowledgements

The authors thank Daniel Veit (Max Planck Institute for Chemical Ecology, Jena, Germany) for providing the modified LI-820 $CO_2$ Gas Analyzer. They also extend their gratitude to Dr. Johan Zicola, Katharina Ziese-Kubon, Jonas Watterott, and Ruth Pilot for their support. The authors acknowledge the funding provided by the Deutscher Akademischer Austauschdienst (grants to Gözde Güney and Doga Cedden). Open access funding enabled and organized by Project DEAL. The graphical abstract was created using BioRender.com, with assistance from Metin Cedden.

## Appendix A. Supplementary data

Supplementary data to this article can be found online at https://doi.org/10.1016/j.ibmb.2024.104165.

## References

Alford, D.V., 1979. Observations on the cabbage stem flea beetle, *Psylliodes chrysocephala*, on winter oil-seed rape in Cambridgeshire. Ann. Appl. Biol. 93, 117–123. https://doi.org/10.1111/j.1744-7348.1979.tb06521.x.

Ankersmit, G.W., 1964. Voltinism and its determination in some beetles of cruciferous crops (phd). Veenman, Wageningen. 64, 1–60.

Arrese, E.L., Soulages, J.L., 2010. Insect fat body: energy, metabolism, and regulation. Annu. Rev. Entomol. 55, 207–225. https://doi.org/10.1146/annurev-ento-112408-085356.

Bao, B., Xu, W.-H., 2011. Identification of gene expression changes associated with the initiation of diapause in the brain of the cotton bollworm, *Helicoverpa armigera*. BMC Genom. 12, 224. https://doi.org/10.1186/1471-2164-12-224.

Bonnemaison & Jourdheuil, 1954. L'altise d'hiver du colza (*Psylliodes chrysocephala* L.). Ann. Epiphyt. (Paris) 4, 345–524.

Benoit, J.B., 2010. Water management by dormant insects: comparisons between dehydration resistance during summer aestivation and winter diapause. In: Arturo Navas, C., Carvalho, J.E. (Eds.), Aestivation: Molecular and Physiological Aspects. Springer, Berlin, Heidelberg, pp. 209–229. https://doi.org/10.1007/978-3-642-02421-4_10.

Benoit, J.B., Denlinger, D.L., 2007. Suppression of water loss during adult diapause in the northern house mosquito, *Culex pipiens*. J. Exp. Biol. 210, 217–226. https://doi.org/10.1242/jeb.02630.

Cedden, D., Güney, G., Debaisieux, X., Scholten, S., Rostás, M., Bucher, G., 2024a. Effective target genes for RNA interference-based management of the cabbage stem flea beetle. Insect Mol. Biol. 1–13. https://doi.org/10.1111/imb.12942, 2024.

Cedden, D., Güney, G., Scholten, S., Rostás, M., 2024b. Lethal and sublethal effects of orally delivered double-stranded RNA on the cabbage stem flea beetle, *Psylliodes chrysocephala*. Pest Manag. Sci. 80, 2282–2293. https://doi.org/10.1002/ps.7494.

Cedden, D., Güney, G., Toprak, U., 2024c. The integral role of de novo lipogenesis in the preparation for seasonal dormancy. Proc. Natl. Acad. Sci. USA 121, e2406194121. https://doi.org/10.1073/pnas.2406194121.

Crowe, J.H., 2007. Trehalose as a "chemical chaperone": fact and fantasy. Adv. Exp. Med. Biol. 594, 143–158. https://doi.org/10.1007/978-0-387-39975-1_13.

Denlinger, D.L., 2002. Regulation of diapause. Annu. Rev. Entomol. 47, 93–122. https://doi.org/10.1146/annurev.ento.47.091201.145137.

Denlinger, D.L., 2022. Insect Diapause. Cambridge University Press, Cambridge. https://doi.org/10.1017/9781108609364.

Edde, P.A., 2022. Arthropod pests of rapeseed (canola) (*Brassica napus* L.). In: Edde, P.A. (Ed.), Field Crop Arthropod Pests of Economic Importance. Academic Press, pp. 140–207. https://doi.org/10.1016/B978-0-12-818621-3.00004-5.

Foray, V., Pelisson, P.-F., Bel-Venner, M.-C., Desouhant, E., Venner, S., Menu, F., Giron, D., Rey, B., 2012. A handbook for uncovering the complete energetic budget in insects: the van Handel's method (1985) revisited. Physiol. Entomol. 37, 295–302. https://doi.org/10.1111/j.1365-3032.2012.00831.x.

Gibbs, A.G., Fukuzato, F., Matzkin, L.M., 2003. Evolution of water conservation mechanisms in Drosophila. J. Exp. Biol. 206, 1183–1192. https://doi.org/10.1242/jeb.00233.

Gill, H.K., Goyal, G., Chahil, G., 2017. Insect diapause: a review. J. Agric. Sci. Technol. 7 https://doi.org/10.17265/2161-6256/2017.07.002.

Glazier, D.S., 2015. Body-mass scaling of metabolic rate: what are the relative roles of cellular versus systemic effects? Biology 4, 187–199. https://doi.org/10.3390/biology4010187.

Güney, G., Toprak, U., Hegedus, D.D., Bayram, Ş., Coutu, C., Bekkaoui, D., Baldwin, D., Heckel, D.G., Hänniger, S., Cedden, D., Mutlu, D.A., Suludere, Z., 2021. A look into Colorado potato beetle lipid metabolism through the lens of lipid storage droplet proteins. Insect Biochem. Mol. Biol. 133, 103473 https://doi.org/10.1016/j.ibmb.2020.103473.

Guo, Z., Qin, J., Zhou, X., Zhang, Y., 2018. Insect transcription factors: a landscape of their structures and biological functions in Drosophila and beyond. Int. J. Mol. Sci. 19, 3691. https://doi.org/10.3390/ijms19113691.

Hahn, D.A., Denlinger, D.L., 2011. Energetics of insect diapause. Annu. Rev. Entomol. 56, 103–121. https://doi.org/10.1146/annurev-ento-112408-085436.

Hahn, D.A., Denlinger, D.L., 2007. Meeting the energetic demands of insect diapause: nutrient storage and utilization. J. Insect Physiol. 53, 760–773. https://doi.org/10.1016/j.jinsphys.2007.03.018.

Hao, K., Jarwar, A.R., Ullah, H., Tu, X., Nong, X., Zhang, Z., 2019. Transcriptome sequencing reveals potential mechanisms of the maternal effect on egg diapause induction of *Locusta migratoria*. Int. J. Mol. Sci. 20 https://doi.org/10.3390/ijms20081974.

Hayward, S.A.L., Pavlides, S.C., Tammariello, S.P., Rinehart, J.P., Denlinger, D.L., 2005. Temporal expression patterns of diapause-associated genes in flesh fly pupae from the onset of diapause through post-diapause quiescence. J. Insect Physiol., Diapause and Biological Clocks 51, 631–640. https://doi.org/10.1016/j.jinsphys.2004.11.009.

Jia, Q., Li, S., 2023. Mmp-induced fat body cell dissociation promotes pupal development and moderately averts pupal diapause by activating lipid metabolism. Proc. Natl. Acad. Sci. USA 120, e2215214120. https://doi.org/10.1073/pnas.2215214120.

Kang, D.S., Cotten, M.A., Denlinger, D.L., Sim, C., 2016. Comparative transcriptomics reveals key gene expression differences between diapausing and non-diapausing adults of *Culex pipiens*. PLoS One 11, e0154892. https://doi.org/10.1371/journal.pone.0154892.

Kankare, M., Parker, D.J., Merisalo, M., Salminen, T.S., Hoikkala, A., 2016. Transcriptional differences between diapausing and non-diapausing *d. Montana* females reared under the same photoperiod and temperature. PLoS One 11, e0161852. https://doi.org/10.1371/journal.pone.0161852.

Kaufmann, O., 1941. Zur Biologie des Rapserdflohes (*Psylliodes chrysocephala* L.). Z. Pflanzenkrankh. Pflanzenpathol. Pflanzenschutz (Vienna) 51, 305–324.

Kikawada, T., Saito, A., Kanamori, Y., Nakahara, Y., Iwata, K., Tanaka, D., Watanabe, M., Okuda, T., 2007. Trehalose transporter 1, a facilitated and high-capacity trehalose transporter, allows exogenous trehalose uptake into cells. Proc. Natl. Acad. Sci. USA 104, 11585–11590. https://doi.org/10.1073/pnas.0702538104.

King, B., Li, S., Liu, C., Kim, S.J., Sim, C., 2020. Suppression of glycogen synthase expression reduces glycogen and lipid storage during mosquito overwintering diapause. J. Insect Physiol. 120, 103971 https://doi.org/10.1016/j.jinsphys.2019.103971.

Kojić, D., Popović, Ž.D., Orčić, D., Purać, J., Orčić, S., Vukašinović, E.L., Nikolić, T.V., Blagojević, D.P., 2018. The influence of low temperature and diapause phase on sugar and polyol content in the European corn borer *Ostrinia nubilalis* (Hbn.). J. Insect Physiol. 109, 107–113. https://doi.org/10.1016/j.jinsphys.2018.07.007.

Koštál, V., 2006. Eco-physiological phases of insect diapause. J. Insect Physiol. 52, 113–127. https://doi.org/10.1016/j.jinsphys.2005.09.008.

Krogh, A., Larsson, B., von Heijne, G., Sonnhammer, E.L., 2001. Predicting transmembrane protein topology with a hidden Markov model: application to complete genomes. J. Mol. Biol. 305, 567–580. https://doi.org/10.1006/jmbi.2000.4315.

Kühsel, S., Brückner, A., Schmelzle, S., Heethoff, M., Blüthgen, N., 2017. Surface area–volume ratios in insects. Insect Sci. 24, 829–841. https://doi.org/10.1111/1744-7917.12362.

Lebenzon, J.E., Denezis, P.W., Mohammad, L., Mathers, K.E., Turnbull, K.F., Staples, J.F., Sinclair, B.J., 2022. Reversible mitophagy drives metabolic suppression in

diapausing beetles. Proc. Natl. Acad. Sci. U.S.A. 119, e2201089119 https://doi.org/10.1073/pnas.2201089119.
Lebenzon, J.E., Torson, A.S., Sinclair, B.J., 2021. Diapause differentially modulates the transcriptomes of fat body and flight muscle in the Colorado potato beetle. Comp. Biochem. Physiol., Part D: Genomics Proteomics 40, 100906. https://doi.org/10.1016/j.cbd.2021.100906.
Lehmann, P., Westberg, M., Tang, P., Lindström, L., Käkelä, R., 2020. The diapause lipidomes of three closely related beetle species reveal mechanisms for tolerating energetic and cold stress in high-latitude seasonal environments. Front. Physiol. 11 https://doi.org/10.3389/fphys.2020.576617.
Liu, Z., Xin, Y., Zhang, Y., Fan, J., Sun, J., 2016. Summer diapause induced by high temperatures in the oriental tobacco budworm: ecological adaptation to hot summers. Sci. Rep. 6, 27443 https://doi.org/10.1038/srep27443.
Ma, H.-Y., Zhou, X.-R., Tan, Y., Pang, B.-P., 2019. Proteomic analysis of adult *Galeruca daurica* (Coleoptera: Chrysomelidae) at different stages during summer diapause. Comp. Biochem. Physiol., Part D: Genomics Proteomics 29, 351–357. https://doi.org/10.1016/j.cbd.2019.01.007.
Masaki, S., 1980. Summer diapause. Annu. Rev. Entomol. 25, 1–25. https://doi.org/10.1146/annurev.en.25.010180.000245.
Matthews, P.G.D., White, C.R., 2012. Discontinuous gas exchange, water loss, and metabolism in *Protaetia cretica* (Cetoniinae, Scarabaeidae). Physiol. Biochem. Zool. Ecol. Evol. Approaches 85, 174–182. https://doi.org/10.1086/664590.
Melicher, D., Torson, A.S., Yocum, G.D., Bosch, J., Kemp, W.P., Bowsher, J.H., Rinehart, J.P., 2024. Metabolic and transcriptomic characterization of summer and winter dormancy in the solitary bee, *Osmia lignaria*. Insect Biochem. Mol. Biol. 166, 104074 https://doi.org/10.1016/j.ibmb.2024.104074.
Numata, H., Shintani, Y., 2023. Diapause in univoltine and semivoltine life cycles. Annu. Rev. Entomol. 68, 257–276. https://doi.org/10.1146/annurev-ento-120220-101047.
Ortega-Ramos, P.A., Coston, D.J., Seimandi-Corda, G., Mauchline, A.L., Cook, S.M., 2022. Integrated pest management strategies for cabbage stem flea beetle (*Psylliodes chrysocephala*) in oilseed rape. Glob. Change Biol. Bioenergy 14, 267–286. https://doi.org/10.1111/gcbb.12918.
Petersen, T.N., Brunak, S., von Heijne, G., Nielsen, H., 2011. SignalP 4.0: discriminating signal peptides from transmembrane regions. Nat. Methods 8, 785–786. https://doi.org/10.1038/nmeth.1701.
Ren, S., Hao, Y.-J., Chen, B., Yin, Y.-P., 2018. Global transcriptome sequencing reveals molecular profiles of summer diapause induction stage of onion maggot. Delia antiqua (Diptera: Anthomyiidae). G3 Bethesda Md 8, 207–217. https://doi.org/10.1534/g3.117.300393.
Rinehart, J.P., Li, A., Yocum, G.D., Robich, R.M., Hayward, S.A.L., Denlinger, D.L., 2007. Up-regulation of heat shock proteins is essential for cold survival during insect diapause. Proc. Natl. Acad. Sci. USA 104, 11130–11137. https://doi.org/10.1073/pnas.0703538104.
Robich, R.M., Denlinger, D.L., 2005. Diapause in the mosquito *Culex pipiens* evokes a metabolic switch from blood feeding to sugar gluttony. Proc. Natl. Acad. Sci. U.S.A. 102, 15912–15917. https://doi.org/10.1073/pnas.0507958102.
Robich, R.M., Rinehart, J.P., Kitchen, L.J., Denlinger, D.L., 2007. Diapause-specific gene expression in the northern house mosquito, *Culex pipiens* L., identified by suppressive subtractive hybridization. J. Insect Physiol., Physiology of Vector Arthropods 53, 235–245. https://doi.org/10.1016/j.jinsphys.2006.08.008.
Såringer, Gy, 1984. Summer diapause of cabbage stem flea beetle, *Psylliodes chrysocephala* L. (Col., Chrysomelidae). J. Appl. Entomol. 98, 50–54. https://doi.org/10.1111/j.1439-0418.1984.tb02683.x.
Saulich, A.Kh, Musolin, D.L., 2018. Summer diapause as a special seasonal adaptation in insects: diversity of forms, control mechanisms, and ecological importance. Entomol. Rev. 97, 1183–1212. https://doi.org/10.1134/S0013873817090019.
Schiesari, L., O'Connor, M.B., 2013. Chapter Eight - diapause: Delaying the developmental clock in response to a changing environment. In: Rougvie, A.E., O'Connor, M.B. (Eds.), Current Topics in Developmental Biology : Developmental Timing. Academic Press, pp. 213–246. https://doi.org/10.1016/B978-0-12-396968-2.00008-7.
Sgolastra, F., Bosch, J., Molowny-Horas, R., Maini, S., Kemp, W.P., 2010. Effect of temperature regime on diapause intensity in an adult-wintering Hymenopteran with obligate diapause. J. Insect Physiol. 56, 185–194. https://doi.org/10.1016/j.jinsphys.2009.10.001.
Shen, X., Liu, W., Wan, F., Lv, Z., Guo, J., 2021. The role of cytochrome p450 4c1 and carbonic anhydrase 3 in response to temperature stress in *Bemisia tabaci*. Insects 12, 1071. https://doi.org/10.3390/insects12121071.
Sinclair, B.J., 2015. Linking energetics and overwintering in temperate insects. J. Therm. Biol., What sets the limit? How thermal limits, performance and preference in ectotherms are influenced by water or energy balance 54, 5–11. https://doi.org/10.1016/j.jtherbio.2014.07.007.
Sinclair, B.J., Marshall, K.E., 2018. The many roles of fats in overwintering insects. J. Exp. Biol. 221, jeb161836 https://doi.org/10.1242/jeb.161836.
Sivčev, L., Graora, D., Sivčev, I., Tomić, V., Dudić, B., 2016. Phenology of cabbage stem flea beetle (*Psylliodes chrysocephala* L.) in oilseed rape. Pestic. Fitomedicina 31, 139–144.
Sømme, L., 1964. Effects of glycerol on cold-hardiness in insects. Can. J. Zool. 42, 87–101. https://doi.org/10.1139/z64-009.
Song, L., Florea, L., 2015. Rcorrector: efficient and accurate error correction for Illumina RNA-seq reads. GigaScience 4, 48. https://doi.org/10.1186/s13742-015-0089-y.
Sporer, T., Körnig, J., Wielsch, N., Gebauer-Jung, S., Reichelt, M., Hupfer, Y., Beran, F., 2021. Hijacking the mustard-oil bomb: how a glucosinolate-sequestering flea beetle copes with plant myrosinases. Front. Plant Sci. 12, 645030 https://doi.org/10.3389/fpls.2021.645030.
Storey, K.B., Storey, J.M., 2012. Aestivation: signaling and hypometabolism. J. Exp. Biol. 215, 1425–1433. https://doi.org/10.1242/jeb.054403.
Tan, Q.-Q., Liu, W., Zhu, F., Lei, C.-L., Wang, X.-P., 2017. Fatty acid synthase 2 contributes to diapause preparation in a beetle by regulating lipid accumulation and stress tolerance genes expression. Sci. Rep. 7, 40509 https://doi.org/10.1038/srep40509.
Tapia, H., Koshland, D.E., 2014. Trehalose is a versatile and long-lived chaperone for desiccation tolerance. Curr. Biol. 24, 2758–2766. https://doi.org/10.1016/j.cub.2014.10.005.
Tixeront, M., Dupuy, F., Cortesero, A.M., Hervé, M.R., 2024. Understanding crop colonization of oilseed rape crops by the cabbage stem flea beetle (*Psylliodes chrysocephala* L. (Coleoptera: Chrysomelidae)). Pest Manag. Sci. 80, 2260–2266. https://doi.org/10.1002/ps.7424.
Toprak, U., Guz, N., Gurkan, M.O., Hegedus, D.D., 2014. Identification and coordinated expression of perilipin genes in the biological cycle of sunn pest, *Eurygaster maura* (Hemiptera: scutelleridae): implications for lipolysis and lipogenesis. Comp. Biochem. Physiol. B Biochem. Mol. Biol. 171, 1–11. https://doi.org/10.1016/j.cbpb.2014.02.001.
Torson, A.S., Bowman, S., Doucet, D., Roe, A.D., Sinclair, B.J., 2023. Molecular signatures of diapause in the Asian longhorned beetle: gene expression. Curr. Res. Insect Sci. 3, 100054 https://doi.org/10.1016/j.cris.2023.100054.
Vig, K., 2003. Data on the biology of cabbage stem flea beetle, *Psylliodes chrysocephalus* (Linnaeus, 1758) (Coleoptera, Chrysomelidae, Alticinae). Commun. Agric. Appl. Biol. Sci. 68, 231–237.
Williams, I.H., 2010. The major insect pests of oilseed rape in europe and their management: an Overview. In: Biocontrol-Based Integrated Management of Oilseed Rape Pests. Springer, Dordrecht, pp. 1–43. https://doi.org/10.1007/978-90-481-3983-5_1.
Willis, C.E., Foster, S.P., Zimmer, C.T., Elias, J., Chang, X., Field, L.M., Williamson, M.S., Davies, T.G.E., 2020. Investigating the status of pyrethroid resistance in UK populations of the cabbage stem flea beetle (*Psylliodes chrysocephala*). Crop Protect. 138, 105316 https://doi.org/10.1016/j.cropro.2020.105316.
Wolda, H., Denlinger, D.L., 1984. Diapause in a large aggregation of a tropical beetle. Ecol. Entomol. 9, 217–230. https://doi.org/10.1111/j.1365-2311.1984.tb00717.x.
Yan, L.Y., Long, C., Ling, L., Yao, T., Bao-Ping, P., 2021. Analysis of the transcriptomes of *Galeruca daurica* (Coleoptera: Chrysomelidae) adults at different summer diapause stages. Acta Entomol. Sin. 64, 1020–1030. https://doi.org/10.16380/j.kcxb.2021.09.002.
Yocum, G.D., Rinehart, J.P., Chirumamilla-Chapara, A., Larson, M.L., 2009. Characterization of gene expression patterns during the initiation and maintenance phases of diapause in the Colorado potato beetle, *Leptinotarsa decemlineata*. J. Insect Physiol. 55, 32–39. https://doi.org/10.1016/j.jinsphys.2008.10.003.
Zhang, X., Du, W., Zhang, J., Zou, Z., Ruan, C., 2020. High-throughput profiling of diapause regulated genes from *Trichogramma dendrolimi* (Hymenoptera: trichogrammatidae). BMC Genom. 21, 864. https://doi.org/10.1186/s12864-020-07285-4.
Zhou, G., Miesfeld, R.L., 2009. Energy metabolism during diapause in *Culex pipiens* mosquitoes. J. Insect Physiol. 55, 40–46. https://doi.org/10.1016/j.jinsphys.2008.10.002.
Zhou, H., Lei, G., Chen, Y., You, M., You, S., 2022. PxTret1-like affects the temperature adaptability of a cosmopolitan pest by altering trehalose tissue distribution. Int. J. Mol. Sci. 23, 9019. https://doi.org/10.3390/ijms23169019.
Zhou, R., Rana, T.M., 2013. RNA-based mechanisms regulating host-virus interactions. Immunol. Rev. 253, 97. https://doi.org/10.1111/imr.12053.
Zhou, X.R., Shan, Y.-M., Tan, Y., Zhang, Z.-R., Pang, B.-P., 2019. Comparative analysis of transcriptome responses to cold stress in *Galeruca daurica* (Coleoptera: Chrysomelidae). J. Insect Sci. Online 19. https://doi.org/10.1093/jisesa/iez109.
Zhu, L., Tian, Z., Guo, S., Liu, W., Zhu, F., Wang, X.-P., 2019. Circadian clock genes link photoperiodic signals to lipid accumulation during diapause preparation in the diapause-destined female cabbage beetles *Colaphellus bowringi*. Insect Biochem. Mol. Biol. 104, 1–10. https://doi.org/10.1016/j.ibmb.2018.11.001.